PAPER

Inorganic–organic nanocomposites of CdSe nanocrystals surface-modified with oligo- and poly(fluorene) moieties†

Ioannis Kanelidis,[a] Aleksandar Vaneski,[b] Daniel Lenkeit,[a] Simon Pelz,[a] Victoria Elsner,[a] Raphaela M. Stewart,[c] Jessica Rodríguez-Fernández,[c] Andrey A. Lutich,[c] Andrei S. Susha,[b] Ralf Theissmann,[d] Sylwia Adamczyk,[e] Andrey L. Rogach*[b] and Elisabeth Holder*[af]

We report a facile grafting-from strategy towards the synthesis of inorganic–organic composites of semiconductor nanocrystals and wide-bandgap polymers. Amino-functional fluorenes have been used as co-ligands for CdSe nanocrystals, thus enabling us to design their surface directly during the synthesis. Highly monodisperse, strongly emitting CdSe nanocrystals have been obtained. Subsequently, a straightforward Yamamoto C–C coupling protocol was used to carry out surface polymerisation, hence modifying CdSe nanocrystals with oligo- and poly(fluorene) moieties. Both amino-fluorene capped CdSe nanocrystals and the resulting nanocrystal–polymer composites were characterized in detail by optical and FT-IR spectroscopy, TEM, AFM, and gel permeation chromatography, showing their potential as novel functional inorganic–organic hybrid materials.

Introduction

The search for novel functional materials with forthcoming applications in photovoltaics and optoelectronics[1–9] as well as in bio-medicine[10] is ongoing. While organic semiconducting polymers[11] are in the focus due to their easy processing and mechanical flexibility, inorganic semiconductor nanocrystals (NCs)[12] are favoured due to their size-dependent optical properties. A new trend in materials design privileges a combination of both, organic and inorganic, components in order to produce hybrid structures combining the preferred properties of both classes of materials.[1,13–18] The direct linkage *via* the so-called "grafting-on" synthetic pathway of the pre-designed functional organic molecules onto the CdSe NCs using poly(thiophenes),[1]

as well as the "grafting-from"-based approach, growing polymer chains on the basis of poly(*para*-phenylene vinylene)[13] or P3HT[18] from the pre-designed CdSe surface, has been reported. In both cases, direct linkage of organic and inorganic components offers the advantage to achieve well-defined materials while avoiding aggregation commonly observed in simple blend[19] or layered[20] systems. Poly(fluorene)s[11,21] in combination with CdSe NCs were found to suppress the polymer's ketodefect in light-emitting diodes[9] and to enhance the efficiency of photodiodes.[5,6] Hybrid structures of wide-bandgap semiconducting polymers and strongly luminescent semiconductor NCs offer favourable perspectives in display technology through a combination of low-cost, large-area processability with a highly saturated emission colour. Further field of possible applications is hybrid organic–inorganic solar cells. In this work, we report a facile grafting-from strategy allowing us to modify CdSe NCs with blue light-emitting wide-bandgap oligo- and poly(fluorene)s. We have used a functional amino-fluorene as a ligand providing end-capping to CdSe NCs directly at the synthesis stage. Subsequently, two different kinds of inorganic–organic nano-composites on the basis of amino-fluorene functionalized CdSe NCs with varying fluorene chain-lengths were obtained *via* a facile nickel(0)-mediated Yamamoto C–C coupling protocol.

Results and discussion

The target amino-functionalized fluorene ligand 6,6′-(2,7-dibromo-9H-fluorene-9,9-diyl)dihexan-1-amine (**Fl-NH₂**) has been obtained by a Gabriel protocol *via* 2,2′-(6,6′-(2,7-dibromo-9H-fluorene-9,9-diyl)*bis*(hexane-6,1-diyl)di*iso*indoline-1,3-dione (**Fl-imide**), starting from 2,7-dibromo-9,9-*bis*(6-bromohexyl)-9

[a]*Functional Polymers Group and Institute of Polymer Technology, University of Wuppertal, Gaußstr. 20, D-42097 Wuppertal, Germany. E-mail: holder@uni-wuppertal.de; Fax: +49 202 439 3880; Tel: +49 202 439 3879*

[b]*Department of Physics and Materials Science, City University of Hong Kong, Tat Chee Avenue, Kowloon, Hong Kong. E-mail: andrey.rogach@cityu.edu.hk; Fax: +852 3442 7830; Tel: +852 3442 9532*

[c]*Photonics and Optoelectronics Group, Department of Physics and CeNS, Ludwig-Maximilians-Universität München, Amalienstr. 54, D-80799 Munich, Germany*

[d]*Faculty of Engineering and Center for Nanointegration Duisburg-Essen (CeNIDE), University of Duisburg-Essen, Bismarckstr. 81, D-47057 Duisburg, Germany*
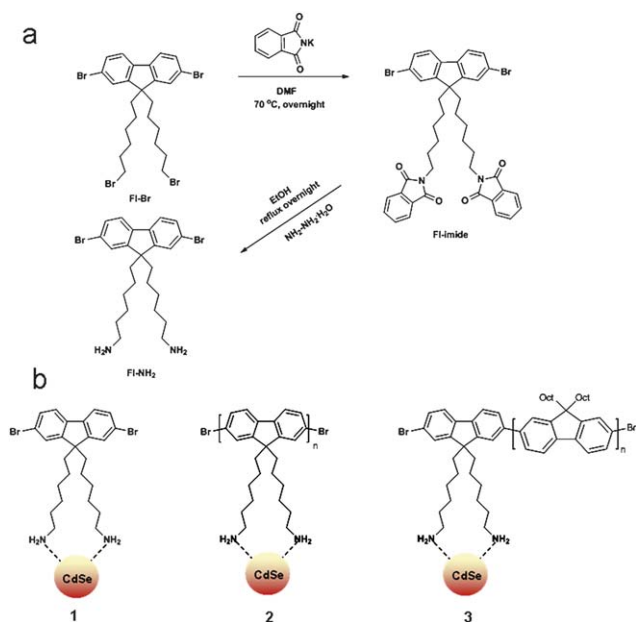
[e]*Macromolecular Chemistry, University of Wuppertal, Gaußstr. 20, D-42097 Wuppertal, Germany*

[f]*Dutch Polymer Institute (DPI), P.O. Box 513, NL-5600 AX Eindhoven, The Netherlands*
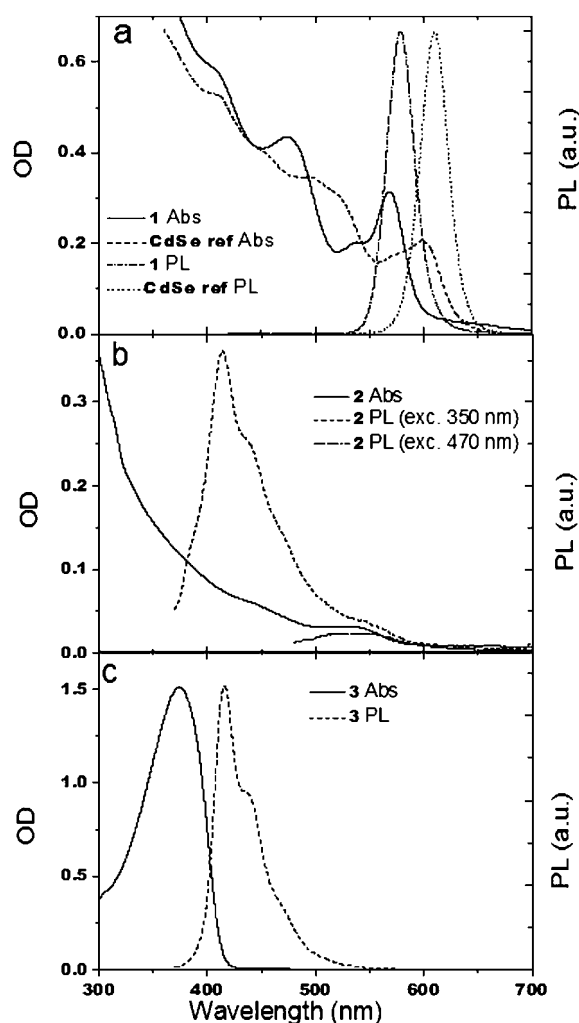
† Electronic supplementary information (ESI) available: AFM and GPC analysis data. See DOI: 10.1039/c0jm03546g

H-fluorene (**Fl-Br**)[22] (Scheme 1a). It was introduced as a co-ligand into the standard synthesis of CdSe NCs,[13] in order to obtain amino-fluorene modified CdSe NCs **1** (Scheme 1b). CdSe NCs synthesized using standard stabilizing ligands *n*-hexadecyl-amine and tetradecylphosphonic acid[13] have been prepared as well and served as a reference sample (**CdSe ref**). The presence of **Fl-NH$_2$** in the reaction mixture strongly slowed down the growth kinetics of CdSe NCs. **CdSe ref** sample has grown to 4.8 nm (estimated from absorption spectra using the sizing curve of ref. 23) in only 3 min, while 3.5 nm sized CdSe NCs have been obtained in the synthesis of **1** after heating for 5 min at the same temperature (Fig. 1a). Fig. 1a also confirms the high quality of **1** in terms of four sharp, well-resolved absorption maxima pointing out on the high degree of monodispersity of NCs, a narrow emission band with a maximum at 580 nm and a sufficiently strong room temperature quantum efficiency of 9% estimated by comparison with Rhodamine 6G. High-resolution TEM image shows high crystallinity of nanoparticles, with lattice planes ascribed to hexagonal CdSe phase (Fig. 2a). The high mono-dispersity of **1** is directly evidenced from TEM (Fig. 2b), with particles readily forming a close-packed monolayer on the TEM grid.

CdSe ref and CdTe NCs **1** have been purified by several cycles of re-dissolving in toluene and subsequent precipitation in methanol in order to remove excessive and weakly bound surface ligands, and FT-IR measurements have been performed. They manifest the linkage of the target ligand **Fl-NH$_2$** on the CdSe surface of **1** by the band at 2359 cm^{-1}, which was assigned to the stretching vibration of the surface-bound NH$_2$ group (Fig. 3a). In the case of **CdSe ref** the band at 2359 cm^{-1}, which may also

Fig. 1 (a) Absorption and photoluminescence (PL, excitation at 400 nm) spectra of **1** (taken after 5 min of NC growth) compared to **CdSe ref** (taken after 3 min of NC growth). (b) Absorption spectrum of **2** and PL spectra of **2** taken at two different excitation wavelengths indicated in the frame. (c) Absorption and PL (excitation at 350 nm) spectra of **3**.


Scheme 1 (a) Synthesis of the target amino-functionalized fluorene ligand 6,6′-(2,7-dibromo-9*H*-fluorene-9,9-diyl)dihexan-1-amine (**Fl-NH$_2$**) by a Gabriel protocol *via* 2,2′-(6,6′-(2,7-dibromo-9*H*-fluorene-9,9-diyl)-*bis*(hexane-6,1-diyl))di*iso*indoline-1,3-dione (**Fl-imide**) starting from 2,7-dibromo-9,9-*bis*(6-bromohexyl)-9*H*-fluorene (**Fl-Br**). (b) Amino-fluorene modified CdSe NCs **1** used to obtain NC–oligofluorene composite **2** and NC–poly(fluorene) composite **3**.

originate from the surface-bound amino-group of *n*-hexadecyl-amine, appears to be much weaker (Fig. 3a). Considered together with the strongly slowed down growth kinetics upon introduc-tion of **Fl-NH$_2$** into the reaction mixture, this observation points out on the higher affinity of **Fl-NH$_2$** towards the CdSe surface as compared to *n*-hexadecylamine. Amines in general have strong coordination ability with CdSe,[1,24,25] while ligands offering chelating groups provide most favourable capping for CdSe NCs.[26] This means that the surface of CdTe NCs **1** has a higher coverage with ligand **Fl-NH$_2$** grafted through its amino-groups as compared to the amount of amino-groups of *n*-hexadecyl-amine bound to the surface of **CdSe ref** NCs.

Gel permeation chromatography (GPC) analysis of **1** does not show any pronounced molecular weight distribution, giving a peak at just 736 Da (see ESI†), which is much lower than the molecular weight of a II–VI NC estimated from the mass of constituting elements for a given NC size (10–12 kDa). This points out that the GPC data, which are obtained relative to poly(methyl methacrylate) standards, cannot be regarded as
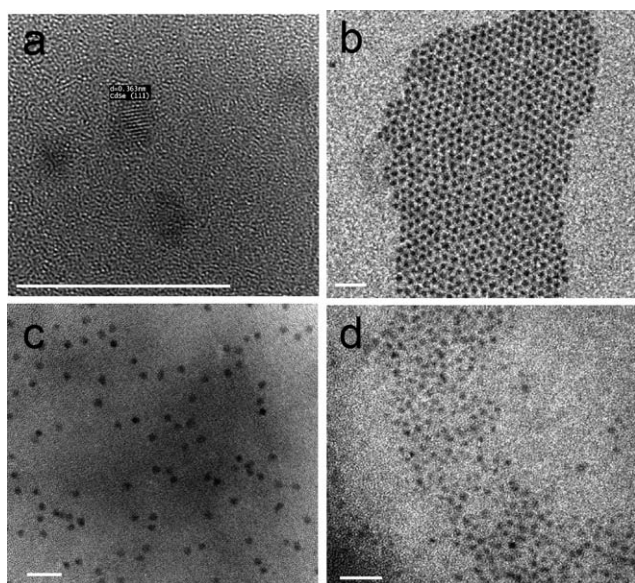
Fig. 2 (a) HRTEM image of CdSe NCs synthesized in the presence of **Fl-NH₂** and TEM images of **1** (b), **2** (c) and **3** (d). The scale bar is 20 nm for all frames.
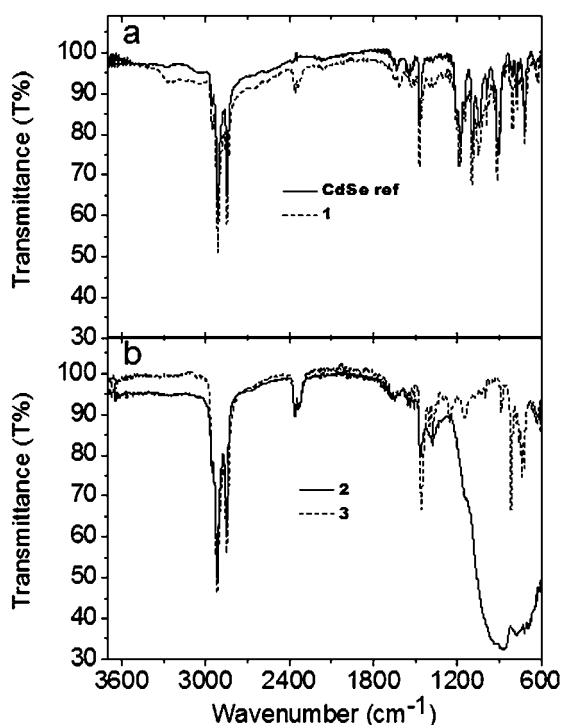
Fig. 3 FT-IR spectra of (a) **CdSe ref** and **1**, and (b) composites **2** and **3**. The linkage of the target ligand **Fl-NH₂** on the CdSe surface is manifested by the band at 2359 cm⁻¹, which was assigned to the stretching vibration of the surface-bound NH₂ group.

absolute values for inorganic NCs, whose hydrodynamic volumes are different and are certainly not comparable to any utilized polymer standards. We have further compared **1** to CdTe NCs of the estimated molecular weight of 6 kDa (ESI†), with the similar result of a strongly underestimated molecular weight

derived from GPC data. This comparison illustrates that for inorganic NCs, GPC molecular weights generally cannot be regarded as absolute even though different elution volumes can be obtained for the different species.

In order to obtain CdSe NCs with oligomerized surface ligands **2** (Scheme 1b), a facile Yamamoto protocol[27] using **1** as a starting material, Ni(0)(COD)₂ as a C–C coupling mediator and THF–toluene 1 : 1 (v/v) as a solvent was applied. After a conventional work-up and purification *via* preparative size exclusion chromatography, composite **2** was obtained in a yield of 71%. Its absorption spectrum (Fig. 1b) clearly reveals the predominant contribution from the inorganic (CdSe NCs) part of the composite. The emission spectra of **2** taken at two different excitation wavelengths (350 nm, where both fluorene moieties and NCs are excited and 470 nm, where excitation of the former is negligible) show the contribution from both constituents, oligofluorene and CdSe NCs (Fig. 1b). The room temperature quantum efficiency of CdSe NCs in **2** is strongly decreased, down to <1%. TEM of **2** shows the presence of non-agglomerated nanoparticles (Fig. 2c). The absence of NC aggregates rules out inter-particle polymerisation, pointing out that the fluorene monomers rather undergo intra-particle oligomerisation at the CdSe NC surface. This is supported by the prevailing contribution of NCs to the absorption of the composite **2**, and further confirms that the surface of **1** is indeed grafted with a sufficient number of **Fl-NH₂**.

GPC elugram pattern of **2** shows the coexistence of two similar species with molecular weights in the range of 1700 Da (ESI†). This molecular weight, which refers to the weight of oligomers formed at the NC surface, shows that the catalytic Yamamoto cycle breaks up after three repeating units of **Fl-NH₂** to undergo intra-particle oligomerisation. The interruption of the polymerisation cycle can be assigned to the limited availability of polymerisable monomer units due to the space limitations at the surface of the NCs. MALDI-TOFMS has been carried out in order to independently analyse the molecular weight of the organic component within the nanocomposite **2**. *m/z* values of a trimer-Br have been identified, supporting the findings of the GPC analysis with respect to the organic counterpart of **2**.

Composite **3** (Scheme 1b) was prepared applying similar Yamamoto procedure[27] but additionally introducing 2,7-dibromo-9,9-dioctyl-9*H*-fluorene as a co-monomer inducing chain growth at the surface of CdSe NCs. After purification, a polymer-like material was obtained in a yield of 83%. Both absorption and emission spectra of **3** are clearly dominated by the poly(fluorene) moieties, and the emission of CdSe NCs is completely quenched (Fig. 1c), while TEM clearly indicates the presence of CdSe cores in the composite (Fig. 2d). FT-IR spectra of both **2** and **3** show a pronounced band at 2359 cm⁻¹ (Fig. 3b), confirming that the linkage between the CdSe NC and the **Fl-NH₂** ligand through the surface-bound NH₂ group remains intact during the polymerisation procedure. The molecular weight distribution of the organic component (M_w = 4738 g mol⁻¹) of **3** determined by GPC analysis (ESI†) elucidates the occurrence of the polymerisation as well. MALDI-TOFMS data for **3** illustrate a broad distribution range of the organic component from the monomer to the dodecamer.

AFM images of films obtained by dip-coating **1** in toluene and **2** and **3** in chloroform on glimmer (Fig. 4) reveal greatly
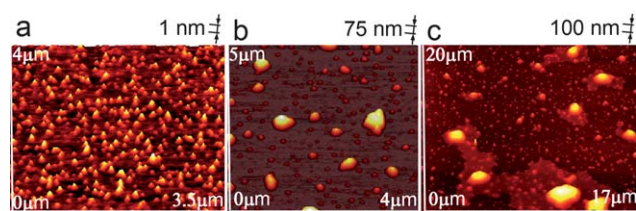
Fig. 4 AFM images of thin films of **1** (a), **2** (b) and **3** (c) dip-coated on glimmer. The surface roughness and the amount of large agglomerates strongly increase for composite material **2** and in particular for **3** as compared to **1**.

increased average surface roughness (see ESI†) of the composite materials (25.5 nm for **2** and 70.9 nm for **3**), as compared to only 0.7 nm for **1**. The clustering is related to the changed surface chemistry of **2** and **3** as compared to **1**, for the samples prepared in the similar way (dip-coated from concentrated solutions). Poly(fluorene) chains have a general tendency to fold/agglomerate,[28] and as they build the major part of the hybrid composite **3** the formation of large clustered agglomerates is in particular observed in this case (Fig. 4c).

Analysing integrated photoluminescence (PL) spectroscopy data (Fig. 1), neither for **2** nor for **3** reliable signatures of energy transfer from polymer to NCs, have been observed. In our previous study we have found out that in organic/inorganic composites resonant energy transfer and charge transfer, from organic to inorganic component, are competing processes.[29] Short separation distances provided by the direct chemical binding may favour efficient charge separation between the organic and inorganic components, leading to PL quenching of both polymer and NCs in the composites. In order to get an insight into the photophysics of the composites synthesized in this work, we have performed time-resolved PL measurements, which showed that CdSe NCs within composites **1** and **3** have considerably faster PL decays compared to the **CdSe ref** NCs (Fig. 5).

This finding is consistent with the PL quenching observed in the steady-state emission measurements (Fig. 1) and supports the hypothesis of charge separation process between CdSe NCs and
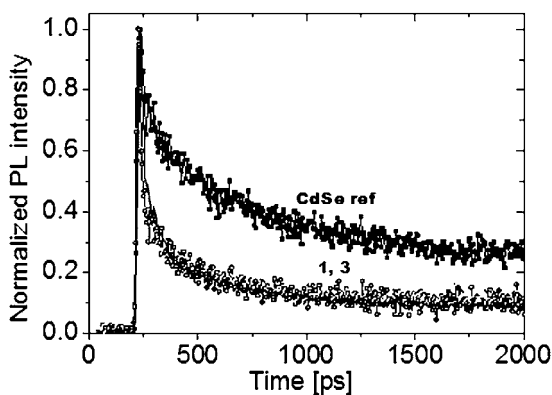
Fig. 5 Photoluminescence decay spectra of CdSe NCs in the samples **CdSe ref**, **1**, and **3**. PL kinetics of CdSe NCs in composites **1** and **3** are coinciding within experimental errors while strongly differing from **CdSe ref**.

fluorene moieties, which renders these hybrid materials promising for photovoltaic devices. Taking into account that PL kinetics of CdSe NCs in composites **1** and **3** are coinciding within experimental errors (Fig. 5), we conclude that optoelectronic properties of the composites are provided by the chemical binding of the monomers to the NC surface and are not affected by the polymerisation procedure.

Experimental section

Instrumentation

UV-vis absorption spectra were taken on a Jasco V-550 spectrophotometer, and time-integrated PL spectra were measured on a Cary Eclipse fluorescence spectrometer. Time-resolved PL measurements were done with a streak camera (Hamamatsu C5680) combined with the spectrometer (Cromex, 40 gr mm^{-1} grating). The frequency doubled output of the mode-locked titanium–sapphire laser (150 fs, 100 kHz) was used as an excitation source at 400 nm. Infrared measurements were conducted on a JASCO FT/IR-4200 Fourier-Transform Spectrometer. Transmission electron microscopy (TEM) images were recorded on a JEOL JEM-1011 electron microscope at an accelerating voltage of 100 kV on samples strongly diluted by chloroform. AFM measurements were performed using a diInnova microscope from Veeco in the tapping mode. The samples were drop casted on glimmer, from chloroform or toluene dispersions of 10 mg mL^{-1} concentration. The silicon cantilevers used were between 215 and 235 μm in length and had a resonance frequency of approximately 84 kHz, while the tip height was between 15 and 20 μm. Gel permeation chromatography (GPC) analysis was carried out on a Jasco AS2055 Plus apparatus using Jasco UV/VIS-2070/75 and Jasco RI-2031 as detectors (GRAM columns, dimethylformamide (DMF) as an eluent with ammonium hexafluorophosphate 5 mM as the salt). For the determination of the molecular weights, a calibration based on poly(methyl methacrylate) standards was applied. Mass spectra were obtained using a Bruker micrOTOF instrument equipped with an electrospray ionization source (ESI-MS) and a Shimadzu Biotech Axima matrix-assisted laser-desorption ionization time-of-flight mass spectrometer (MALDI-TOFMS). MALDI-TOF samples were prepared by drop-casting THF solutions of the composites without the addition of a matrix. ^{1}H and ^{13}C-NMR spectra were recorded in deuterated chloroform (CDCl$_3$) with TMS as a internal standard on Bruker Avance III 600 Fourier Transform nuclear resonance spectrometer. The chemical shift δ is given in ppm. Elemental analyses were performed by means of the Vario Elemental EL analyser. For the purification of the monomers by means of column chromatography silica gel of particle size 50–200 mesh was utilized as the stationary phase.

Materials

All reactions were carried out under inert conditions (argon). 1,6-Dibromohexane, tetrabutylammonium bromide, potassium phthalimide, *bis*(1,5-cyclooctadiene)nickel(0) and bipyridine were purchased from Acros, hydrazine monohydrate and 1,5-cyclooctadiene from Aldrich, 2,7-dibromofluorene from Synthon and bromobenzene from Merck. 2,7-Dibromo-9,9′-*bis*(6-bromohexyl)-9*H*-fluorene[30] and composites **2** and **3**[31]

were synthesized according to literature known procedures. All polymerisations were performed in extra dry THF and toluene added in a 1 : 1 (v/v) proportion.

Synthesis of the monomers

2,7-Dibromo-9,9′-*bis*(6-bromohexyl)-9*H*-fluorene[30]**.** A white solid was obtained (6.78 g, 69%). Found C, 46.86; H, 4.75%. Anal. Calc. for $C_{25}H_{30}Br_4$: C, 46.19; H, 4.65%; UV-vis: λ_{max} (CHCl₃)/nm (log ε [L × mol⁻¹ × cm⁻¹]) 283 (4.47), 316 (4.31); emission: λ_{max} (CHCl₃)/nm 329; IR (ν_{max}/cm⁻¹): 2925 (m, CH₂, stretching), 2850 (m, CH₂, stretching), 1568 (w, C=C, stretching), 1460 (m, CH₂, scissor), 1446 (s, C–H, deformation), 810 (s, aromatic C–H, out-of-plane deformation); ¹H-NMR (CDCl₃, 600 MHz): δ (ppm): 0.56–0.64 (m, 4H, CH₂), 1.04–1.12 (m, 4H, CH₂), 1.17–1.24 (m, 4H, CH₂), 1.64–1.71 (m, 4H, CH₂), 1.91–1.95 (m, 4H, CH₂), 3.29 (t, 4H, CH₂–Br), 7.41–7.56 (m, 6H, arom.); ¹³C-NMR (CDCl₃, 600 MHz): δ (ppm): 152.16, 139.05, 130.06, 126.10, 121.57, 121.19 (arom.), 55.54 (⬡), 39.95, 33.72, 32.59, 28.92, 27.72, 23.45 (aliph.); ESI-MS *m/z* calcd $C_{25}H_{30}AgBr_4$ 758; found 758.8.

2,2′-(6,6′-(2,7-Dibromo-9*H*-fluorene-9,9-diyl)*bis*(hexane-6,1-diyl))di*iso*indoline-1,3-dione[32]**.** 2,7-Dibromo-9,9′-*bis*(6-bromohexyl)-9*H*-fluorene (1 g, 1.54 mmol) was added into a DMF solution (30 mL) of potassium phthalimide (1.426 g, 7.7 mmol). The reaction mixture was kept at 70 °C for 24 hours and allowed to cool down to room temperature. CHCl₃ was added to the reaction mixture and extracted with water (3 × 50 mL). The organic phase was washed with a 0.2 M solution of NaOH (1 × 50 mL) and water (1 × 50 mL), dried over MgSO₄ and the solvent was removed by reduced pressure. The resulting yellowish oil was purified by column chromatography (silica, *n*-hexane–ethyl acetate 3 : 1) yielding a white solid (0.74 g, 62%). Found C, 62.98; H, 4.77; N, 3.24%. Anal. Calc. for $C_{41}H_{38}Br_2N_2O_4$: C, 62.93; H, 4.89; N, 3.58%; UV-vis: λ_{max} (CHCl₃)/nm (log ε [L × mol⁻¹ × cm⁻¹]) 283 (4.55), 313 (4.36); emission: λ_{max} (CHCl₃)/nm 328; IR (ν_{max}/cm⁻¹): 2920 (m, CH₂, stretching), 2854 (m, CH₂, stretching), 1700 (s, C=O, stretching), 1400 (m, C–H, deformation), 1050 (m, C–N, stretching), 720 (s, C–C, skeleton); ¹H-NMR (CDCl₃, 600 MHz): δ (ppm): 0.56–0.59 (m, 4H, CH₂), 0.84–0.91 (m, 4H, CH₂), 1.22–1.29 (m, 4H, CH₂), 1.48–1.54 (m, 4H, CH₂), 1.87–1.91 (m, 4H, CH₂), 3.55–3.58 (t, 4H, N–CH₂), 7.41–7.51 (m, 6H, arom.), 7.66–7.83 (m, 6H, arom.); ¹³C-NMR (CDCl₃, 600 MHz): δ (ppm): 168.34 (C=O), 157.77, 152.25, 139.04, 133.75, 132.17, 130.24, 126.08, 123.1, 121.5, 121.19 (arom.), 55.55 (⬡), 40.07, 37.89, 31.82, 29.46, 28.47, 26.49, 23.55, 20.99 (aliphat.); ESI-MS *m/z* calcd $C_{41}H_{38}Br_2N_2O_4$ (M + H)²⁺ 392.3; found 393.

2,7-Dibromo-9,9′-*bis*(6-aminohexyl)-9*H*-fluorene[32]**.** Hydrazinolysis of 2,2′-(6,6′-(2,7-dibromo-9*H*-fluorene-9,9-diyl)*bis*(hexane-6,1-diyl))di*iso*indoline-1,3-dione (0.74 g, 0.95 mmol) occurred by dissolving it in 99.8% ethanol and hydrazine monohydrate (0.2 mL, 4.13 mmol). The reaction system was refluxed overnight and subsequently allowed to cool down to room temperature, washed with brine (1 × 90 mL) and its pH adjusted to 12 by means of a 50% w/w NaOH solution (30 mL). The organic phase was extracted with CH₂Cl₂ (2 × 100 mL), dried over Na₂SO₄ and the

solvent was removed by reduced pressure. A brownish solid was obtained (0.39 g, 49%). Found C, 57.49; H, 7.14; N, 4.48%. Anal. Calc. for $C_{25}H_{34}Br_2N_2$: C, 57.48; H, 6.56; N, 5.36%; UV-vis: λ_{max} (CHCl₃)/nm (log ε [L × mol⁻¹ × cm⁻¹]) 283 (3.78), 313 (3.52); emission: λ_{max} (CHCl₃)/nm 324; IR (ν_{max}/cm⁻¹): 3352 (w, N–H, stretching), 2920 (s, CH₂, stretching), 2850 (s, CH₂, stretching), 1568 (m, N–H, scissoring), 1448 (s, C–H, deformation), 1056 (m, C–N, stretching), 1003 (m, C–C, skeleton), 808 (s, N–H, out-of-plane bending), 724 (m, C–C, skeleton); ¹H-NMR (CDCl₃, 600 MHz): δ (ppm): 0.56–0.63 (m, 4H, CH₂), 0.83–0.89 (m, 4H, CH₂), 1.07 (t, 4H, CH₂), 1.25 (m, 4H, CH₂), 1.89–1.93 (m, 4H, CH₂), 2.55 (t, 4H, N–CH₂), 7.43–7.52 (m, 6H, arom.); ¹³C-NMR (CDCl₃, 600 MHz): δ (ppm): 152.41, 139.08, 130.22, 127.25, 126.15, 121.15 (arom.), 55.64 (⬡), 42.11, 40.07, 33.69, 29.65, 26.44, 23.61 (aliphat.); ESI-MS *m/z* calcd $C_{25}H_{34}Br_2N_2$ (M + H)⁺ 523.1; found 523.1.

Synthesis of nanocomposites

Nanocomposite 1. 0.21 g (0.79 mmol) Cd(CH₃COO)₂·2H₂O, 2.75 g (11.51 mmol) *n*-hexadecylamine, 0.75 g (2.71 mmol) tetradecylphosphonic acid and 0.94 g (0.18 mmol) 2,7-dibromo-9,9′-*bis*(6-aminohexyl)-9*H*-fluorene were heated under argon to 270 °C. After formation of a transparent solution 0.4 g of selenium in 4 g of *tris-n*-octylphosphine were added *via* a septum. After 5 minutes of heating under argon at 270 °C, the reaction was stopped and NCs were purified by several cycles of precipitation with methanol and redissolution in toluene.

Synthesis of nanocomposites 2 and 3 – general procedure. Composite **1** alone or with 2,7-dibromo-9,9′-dioctyl-9*H*-fluorene,[33] Ni(COD)₂, 2,2′-bipyridine and 1,5-cyclooctadiene were added together in a Schlenk tube. Subsequently, a THF–toluene 1 : 1 mixture (20 mL in total) was added to the reaction system and was allowed to stir for 3 days at 90 °C. 3 Hours before stopping the reaction, 0.05 mL of bromobenzene were added and after cooling down to room temperature the reaction solution was taken with chloroform and washed with 2 N HCl (1 × 100 mL), saturated NaHCO₃ solution (1 × 50 mL) and water (2 × 100 mL). The organic phase was dried over Na₂SO₄ and the solvent removed by reduced pressure. The residue was isolated as such (composite **2**) or was dissolved in chloroform (1–2 mL) and precipitated in methanol (300 mL) in the case of composite **3** and further purified over size exclusion chromatography (Biobeads). IR (ν_{max}/cm⁻¹): 2955 (w, CH₂, stretching), 2911 (s, CH₂, stretching), 2847 (m, CH₂, stretching), 2359 (w, NH₂ surface-bound, stretching), 2341 (w, NH₂ surface-bound, stretching), 1526 (w, N–H, scissoring), 1468 (m, C–H, deformation), 1188 (m, C–N, stretching), 1095 (m, C–N, stretching), 916 (m, C–C, skeleton).

Nanocomposite 2. **1** (0.052 g, 46.1 × 10⁻⁷ mmol), Ni(COD)₂ (0.005 g, 0.018 mmol), 2,2′-bipyridine (0.003 g, 0.19 mmol), COD (0.01 mL, 0.08 mmol). Red-particle like material (0.037 g, 71%). UV-vis: λ_{max} (CHCl₃)/nm (log ε [L × mol⁻¹ × cm⁻¹]): 540 (3.07); emission: λ_{max} (CHCl₃)/nm: 413, 545; IR (ν_{max}/cm⁻¹): 2915 (s, CH₂, stretching), 2851 (m, CH₂, stretching), 2351 (w, NH₂ surface-bound, stretching), 2330 (w, NH₂ surface-bound, stretching), 1461 (w, C–H, deformation), 880 (s (br), N–H

2660 | *J. Mater. Chem.*, 2011, **21**, 2656–2662

This journal is © The Royal Society of Chemistry 2011

out-of-plane bending); ^{1}H-NMR (CDCl$_3$, 600 MHz): δ (ppm): 2.76 (s, N–CH$_2$), 1.95–1.88 (m, CH$_2$), 1.71–1.64 (m, CH$_2$), 1.62–1.52 (m, CH$_2$), 1.28 (s, aliphatic), 0.90 (t, CH$_2$). GPC (g mol^{-1}): M_n: 1276, M_w: 1736, M_w/M_n: 1.36. MALDI-TOFMS (m/z): 1166.6 (**Fl-NH$_2$-trimer-Br**).

Nanocomposite 3. 2,7-Dibromo-9,9′-dioctyl-9H-fluorene (0.06 g, 0.109 mmol), **1** (0.052 g, 9.2 × 10^{-7} mmol), Ni(COD)$_2$ (0.072 g, 0.26 mmol), 2,2′-bipyridine (0.037 g, 0.24 mmol), COD (0.03 mL, 0.24 mmol). Red-particle like material (0.1 g, 83%). UV-vis: $λ_{max}$ (CHCl$_3$)/nm (log $ε$ [L × mol^{-1} × cm^{-1}]): 375, (4.54); emission: $λ_{max}$ (CHCl$_3$)/nm: 414, 438; Eg$_{sol}$: 2.94; $Φ_{sol}$: 0.63; IR ($ν_{max}$/cm^{-1}): 2919 (s, CH$_2$, stretching), 2851 (m, CH$_2$, stretching), 2359 (w, NH$_2$ surface-bound, stretching), 2334 (w, NH$_2$ surface-bound, stretching), 1451 (m, C–H, deformation), 1145 (m, C–N, stretching), 815 (m, aromatic C–H, out-of-plane deformation), 739 (m, C–C, skeletal); ^{1}H-NMR (CDCl$_3$, 600 MHz): δ (ppm): 7.74 (s, aromatic), 7.57–7.53 (quintet, aromatic), 7.48 (d, aromatic), 7.46 (d, aromatic), 4.33 (m, P–CH$_2$, tetradecylphosphonic acid), 3.83 (t, N–CH$_2$, n-hexadecylamine), 1.46 (s, CH$_2$), 1.28 (s, CH$_2$), 1.07 (s, CH$_2$), 0.99–0.97 (d, CH$_2$), 0.89 (m, CH$_3$); GPC (g mol^{-1}): M_n: 3718, M_w: 4738, M_w/M_n: 1.27. MALDI-TOFMS (m/z): 387.4 (monomer), 778.0 (dimer), 830 (monomer-ligand-Br), 1166.6 (trimer), 1556.2 (tetramer), 1943.6 (pentamer), 2332.9 (hexamer), 2722.0 (heptamer), 3109.2 (octamer), 3497.1 (nonamer), 3888.0 (decamer), 4275.6 (undecamer), 4663.9 (dodecamer).

Reference materials: CdSe ref NCs. 0.21 g (0.79 mmol) Cd(CH$_3$COO)$_2$·2H$_2$O, 2.75 g (11.51 mmol) n-hexadecylamine, and 0.75 g (2.71 mmol) tetradecylphosphonic acid were heated under argon at 270 °C. After formation of a transparent solution 0.4 g of selenium in 4 g of $tris$-n-octylphosphine were added via a septum. After 3 minutes of heating under argon at 270 °C, the reaction was stopped and NCs were purified by several cycles of precipitation with methanol and redissolution in toluene.

IR ($ν_{max}$/cm^{-1}): 2955 (w, CH$_2$, stretching), 2911 (s, CH$_2$, stretching), 2843 (s, CH$_2$, stretching), 2362 (vw, NH$_2$ surface-bound, stretching), 1637 (w, P–OH, deformation), 1540 (w, N–H, scissoring), 1468 (m, C–H, deformation), 1175 (m, C–N, stretching), 1088 (m, P=O, stretching), 1041 (m, C–C, skeleton), 897 (m, C–C, skeleton), 711 (m, C–C, skeleton).

Conclusions

In conclusion, highly monodisperse, crystalline, strongly emitting CdSe nanoparticles surface-modified by amino-fluorene moieties have been synthesized by a one-step reaction using 6,6′-(2,7-dibromo-9H-fluorene-9,9-diyl)dihexan-1-amine (**Fl-NH$_2$**) as a co-ligand. FT-IR data confirm the formation of surface bond of ligand's NH$_2$ groups and the CdSe surface. **Fl-NH$_2$**-modified CdSe NCs have been used as a starting material in a straight-forward Yamamoto C–C coupling protocol to obtain oligo-fluorene capped CdSe NCs as well as non-aggregated CdSe NC surrounded by poly(fluorene). Emission of CdSe NCs has been strongly quenched, the effect which we ascribe to the charge separation between CdSe NCs and fluorene moieties. The synthetic approach demonstrated here provides a general synthetic pathway to polymer-capped semiconductor NCs, where altering the polymer structure, the NC size and

composition and the chemical linking of the two components, the key parameters of the hybrid inorganic–organic composites (e.g. relative and absolute HOMO/LUMO levels, polymer–nanoparticle distance, film morphology) can be altered in a controlled way. The high degree of control over the electronic and optical properties of hybrid inorganic–organic composites provided by this synthetic concept is a key issue for successful implementation of hybrid materials in photovoltaic and opto-electronic applications.

Acknowledgements

References

1 J. Liu, T. Tanaka, K. Sivula, A. P. Alivisatos and J. M. J. Frechet, *J. Am. Chem. Soc.*, 2004, **126**, 6550–6551.

2 G. Zotti, B. Vercelli, A. Berlin, M. Pasini, T. L. Nelson, R. D. McCullough and T. Virgili, *Chem. Mater.*, 2010, **22**, 1521–1532.

3 J. Nei de Freitas, I. R. Grova, L. C. Akcelrud, E. Arici, N. S. Sariciftci and A. F. Nogueira, *J. Mater. Chem.*, 2010, **20**, 4845–4853.

4 D. Aldakov, T. Jiu, M. Zagorska, R. de Bettignies, P.-H. Jouneau, A. Pron and F. Chandezon, *Phys. Chem. Chem. Phys.*, 2010, **12**, 7497–7505.

5 P. Wang, A. Abrusci, H. M. P. Wong, M. Svensson, M. R. Andersson and N. C. Greenham, *Nano Lett.*, 2006, **6**, 1789–1793.

6 S. Dayal, N. Kopidakis, D. C. Olson, D. S. Ginley and G. Rumbles, *Nano Lett.*, 2010, **10**, 239–242.

7 H. V. Demir, S. Nizamoglu, T. Ozel, E. Mutlugun, I. O. Huyal, E. Sari, E. Holder and N. Tian, *New J. Phys.*, 2007, **9**, 362–374.

8 A. L. Rogach, N. Gaponik, J. M. Lupton, C. Bertoni, D. E. Gallardo, S. Dunn, N. Li Pira, M. Paderi, P. Repetto, S. G. Romanov, C. O'Dwyer, C. M. Sotomayor Torres and A. Eychmüller, *Angew. Chem., Int. Ed.*, 2008, **47**, 6538–6549.

9 C.-H. Yang, C. J. Bhongale, C.-H. Chou, S.-H. Yang, C.-N. Lo, T.-M. Chen and C.-S. Hsu, *Polymer*, 2007, **48**, 116–128.

10 G. Jiang, A. S. Susha, A. A. Lutich, F. D. Stefani, J. Feldmann and A. L. Rogach, *ACS Nano*, 2009, **3**, 4127–4131.

11 (a) A. C. Grimsdale, K. L. Chan, R. E. Martin, P. G. Jokisz and A. B. Holmes, *Chem. Rev.*, 2009, **109**, 897–1091; (b) E. Tekin, E. Holder, D. Kozodaev and U. S. Schubert, *Adv. Funct. Mater.*, 2007, **17**, 277–284; (c) E. Tekin, H. Wijlaars, E. Holder, D. A. M. Egbe and U. S. Schubert, *J. Mater. Chem.*, 2006, **16**, 4294–4298.

12 *Semiconductor Nanocrystal Quantum Dots: Synthesis, Assembly, Spectroscopy and Applications*, ed. A. L. Rogach, Springer, Wien, New York, 2008.

13 H. Skaff, K. Sill and T. Emrick, *J. Am. Chem. Soc.*, 2004, **126**, 11322–11325.

14 E. Holder, N. Tessler and A. L. Rogach, *J. Mater. Chem.*, 2008, **18**, 1064–1078.

This journal is © The Royal Society of Chemistry 2011

J. Mater. Chem., 2011, **21**, 2656–2662 | 2661

15 J. De Girolamo, P. Reiss and A. Pron, *J. Phys. Chem. C*, 2007, **111**, 14681–14688.

16 N. I. Hammer, T. Emrick and M. D. Barnes, *Nanoscale Res. Lett.*, 2007, **2**, 282–290.

17 Z. Lin, *Chem.–Eur. J.*, 2008, **14**, 6294–6301.

18 S. Dayal, N. Kopidakis, D. C. Olson, D. S. Ginley and G. Rumbles, *J. Am. Chem. Soc.*, 2009, **131**, 17726–17727.

19 O. Solomeshch, A. Kigel, A. Saschiuk, V. Medvedev, A. Aharoni, A. Razin, Y. Eichen, U. Banin, E. Lifshitz and N. Tessler, *J. Appl. Phys.*, 2005, **98**, 074310–074311.

20 A. A. Lutich, A. Pöschl, G. Jiang, F. D. Stefani, A. S. Susha, A. L. Rogach and J. Feldmann, *Appl. Phys. Lett.*, 2010, **96**, 083109–083111.

21 A. C. Grimsdale and K. Müllen, in *Advances in Polymer Science*, Springer Verlag, Berlin, Heidelberg, 2006, vol. 199, pp. 1–82.

22 B. Liu, S. Wang, G. C. Bazan and A. Mikhailovsky, *J. Am. Chem. Soc.*, 2003, **125**, 13306–13307.

23 W. W. Yu, L. Qu, W. Guo and X. Peng, *Chem. Mater.*, 2003, **15**, 2854–2860.

24 D. V. Talapin, A. L. Rogach, A. Kornowski, M. Haase and H. Weller, *Nano Lett.*, 2001, **1**, 207–211.

25 C. Bullen and P. Mulvaney, *Langmuir*, 2006, **22**, 3007–3013.

26 C. Querner, A. Benedetto, R. Demadrille, P. Rannou and P. Reiss, *Chem. Mater.*, 2006, **18**, 4817–4826.

27 A. Tsami, X.-H. Yang, F. Galbrecht, T. Farrell, H. Li, S. Adamczyk, R. Heiderhoff, L. J. Balk, D. Neher and E. Holder, *J. Polym. Sci., Part A: Polym. Chem.*, 2007, **45**, 4773–4785.

28 M. Grell, D. D. C. Bradley, G. Ungar, J. Hill and K. S. Whitehead, *Macromolecules*, 1999, **32**, 5810–5817.

29 A. A. Lutich, G. Jiang, A. S. Susha, A. L. Rogach, F. D. Stefani and J. Feldmann, *Nano Lett.*, 2009, **9**, 2636–2640.

30 E. P. Woo, M. Inbasekaran, W. R. Shiang and G. R. Roof, WO/05184, 1997.

31 L. Kinder, J. Kanicki and P. Petroff, *Synth. Met.*, 2004, **146**, 181–185.

32 V. Marin, E. Holder, R. Hoogenboom and U. S. Schubert, *Macromol. Rapid Commun.*, 2004, **25**, 793–798.

33 B. Liu, B. S. Gaylord and G. C. Bazan, *J. Am. Chem. Soc.*, 2003, **125**, 6705–6714.